



## Energy dissipation mechanism and damage model of marble failure under two stress paths

Liming Zhang

*College of Science, Qingdao Technological University, Qingdao, Shandong 266033, China;*

*dryad\_274@163.com*

*Co-operative Innovation Center of Engineering Construction and Safety in Shandong Peninsula blue economic zone, Qingdao Technological University; Qingdao, Shandong 266033, China;*

*dryad\_274@163.com*

Mingyuan Ren, Shaoqiong Ma, Zaiquan Wang

*College of Science, Qingdao Technological University, Qingdao, Shandong 266033, China;*

*Email: myfy90@163.com, msq\_qq@163.com, zqw4521@163.com*

---

**ABSTRACT.** Marble conventional triaxial loading and unloading failure testing research is carried out to analyze the elastic strain energy and dissipated strain energy evolutionary characteristics of the marble deformation process. The study results show that the change rates of dissipated strain energy are essentially the same in compaction and elastic stages, while the change rate of dissipated strain energy in the plastic segment shows a linear increase, so that the maximum sharp point of the change rate of dissipated strain energy is the failure point. The change rate of dissipated strain energy will increase during unloading confining pressure, and a small sharp point of change rate of dissipated strain energy also appears at the unloading point. The damage variable is defined to analyze the change law of failure variable over strain. In the loading test, the damage variable growth rate is first rapid then slow as a gradual process, while in the unloading test, a sudden increase appears in the damage variable before reaching the rock peak strength. According to the deterioration law of damage and the impact of confining pressure on the elastic modulus, a rock damage constitutive model is established, which has a better fitting effect on the data in the loading and unloading failure processes.

**KEYWORDS.** Marble; Energy evolution; Damage variable; Constitutive equation.

---

### INTRODUCTION

**R**ock mass, which is a typical non-homogeneous material, shows initial damage during formation and long geological processes. In the rock loading process, internal damage continues to accumulate, micro-cracks are expanded and aggregated, and these ultimately connect to cause rock failure. Damage characterizes the rock

---

failure process from the microscopic perspective. Cao et al. [1] considered that rocks with partial damage may also withstand the loads, and the rock damage statistical model was established accordingly. Qin et al. [2] build a damage constitutive equation based on the rock uniaxial-compression. Ha et al. [3] studied rock failure mechanism under unloading stress path. Huang et al. [4, 5] believed that rock unloading damage had obvious tension-shear failure characteristics. Wu and Zhang [6] regarded failure parameter as one of the parameters of rock mechanic characteristics. Shi et al. [7] believed that the rock deformation curve was consistent with Weibull distribution, and Hoek-Brown's guideline was used to establish the rock damage model. Zhang et al. [8] proposed the concept of basic damage, and provided the damage equation under the condition of rock uniaxial compression. Xu and Wei [9] used the proportion of damaged micro-unit volume accounting for the total as the damage variable to establish a rock failure statistical model.

In recent years, the energy perspective has become a new perspective for rock failure research. Chen et al. [10] conducted rock failure experiments before and after the peak strength. They proposed a new index of rock energy discrimination. Xu et al. [11] studied the energy consumption characteristics of sandstone under loading and unloading stress paths. They draw that the various energy indicators are elevated with the larger confining pressure. Jin et al. [12] analyzed the change law of dissipated energy in the uniaxial cyclic loading and unloading processes, and used the energy method to determine the rock damage thresholds in different loading paths. Based on the relationship between damage and energy dissipation, Du [13] defined the failure variable and established the damage mechanics model for structured soils. Hua and You [14] observed that without external force, the elastic energy accumulated in the rock loading process may release itself to cause failure. The rock three-point bending tests conducted by Zhou et al. [15] showed that the strain energy density would show a nonlinear increase with the increase of loading rate. Gaziev [16] believed that the fracture energy caused by the failure of rock in brittle materials was closely related to stress state. Xie et al. [17] believed that the essence of rock failure is the damage caused by energy dissipation. Liu et al. [18] draw a conclusion that most of external work was converted into rock elastic strain energy before yielding. However, the dissipation strain energy increased rapidly after yielding. Zhang et al. [19] believed that the rate of dissipated strain energy change went up with the unloading rate increase.

The above studies analyze rock failure from the perspective of damage, but there is currently a lack of combining energy dissipation mechanism to study the characteristics of rock failure, and research regarding the rock failure constitutive model under triaxial loading and unloading paths is scarce. In this study, by analyzing energy accumulation, dissipation and release characteristics throughout the entire process of marble deformation under loading and unloading stress paths, the damage variable is defined from the perspective of energy dissipation, and a rock failure mechanics model is established.

## TEST STRESS PATHS

The test is completed on MTS rock testing machine. Marble rock blocks are processed with a diameter of 50 mm and height of 100 mm. The rock sample precision meets the requirements of the rock mechanic test. In order to ensure the uniformity of the rock sample, the screen is conducted in two steps: first the significantly-jointed rock samples are removed, then a rock sample with the wave velocity of 4000-4400 m/s is selected.

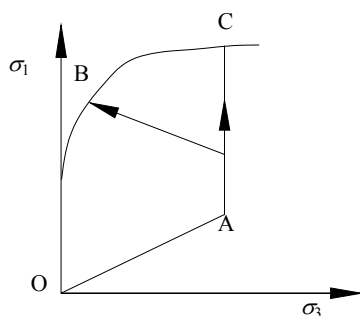


Figure 1: Stress paths of marble loading and unloading test.

There are two stress paths in the test, i.e. the conventional triaxial loading and unloading (Fig. 1). OAC is the conventional triaxial test path, and OAB is the test path with confining pressure unloading, of which the respective unloading rates of confining pressure are 0.2, 0.4 and 0.8 MPa/s.



### ENERGY DISSIPATION CHARACTERISTICS OF MARBLE FAILURE PROCESS

#### Calculation method of energy

According to the energy principle, the acting of external forces on the test system is as shown below:

$$U = U^d + U^e \tag{1}$$

where

$U$  is the total work done by external force on the rock specimens,

$U^d$  is the dissipated strain energy,

$U^e$  is the elastic strain energy.

The calculation relationship is shown in Fig. 2, [17].

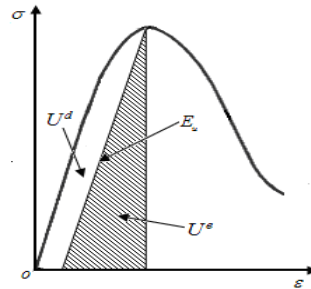


Figure 2: The numerical relationship between the dissipated strain energy and the elastic strain energy [17].

#### Analysis of energy dissipation characteristics

Fig. 3 shows the relation between the marble axial stress, strain energy and axial strain at different stress paths. The energy curve has the following characteristics: (1) Compaction stage: the dissipated strain energy is very small, while elastic strain energy grows slowly. (2) Elastic stage: external force continues to work, elastic strain energy is developed approximately parallel to total strain energy, while the dissipated strain energy increases slowly. It is believed that the elastic stage is the stage of energy accumulation, when most of the energy absorbed by the rock specimens can be stored as elastic strain energy. (3) Pre-peak plastic stage: total strain energy continues to increase. The propagation of internal cracks must dissipate a large amount of external force work, so that the energy is absorbed and begins converting into surface energy for crack propagation, and the growth rate of the dissipated strain energy is increased significantly, while that of the elastic strain energy is slowed. (4) Post-peak stage: from the peak point to stress drop point, a large number of micro-cracks are propagated and accumulated until the emergence of macroscopic rupture occurs, and this must overcome the work of the frictional force, resulting in a substantial increase in dissipated strain energy. When the stress drops sharply, the internally accumulated elastic strain energy is released rapidly, causing rock failure.

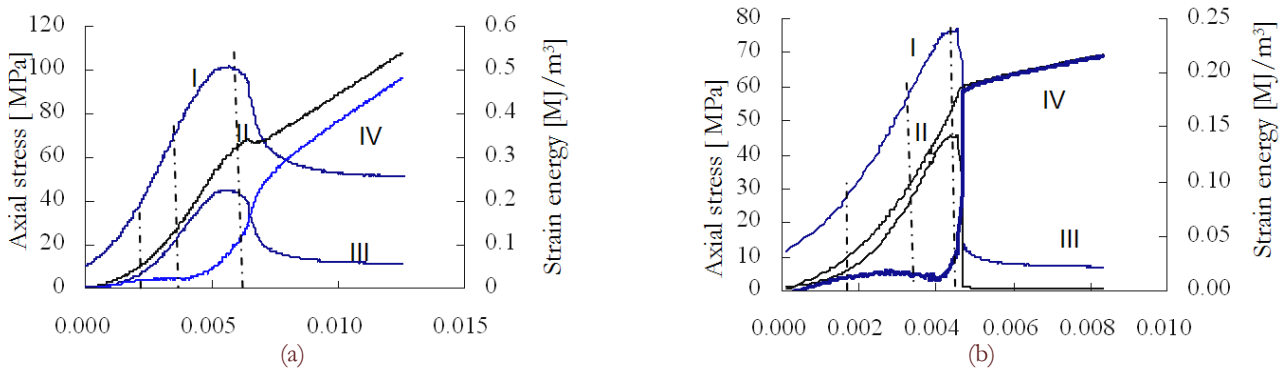


Figure 3: Energy change curves under two stress paths (confining pressure: 10 MPa): (a) The conventional triaxial loading test (b) The conventional triaxial unloading test (I Axial stress, II Absorbed total strain energy, III Elastic strain energy, IV Dissipated strain energy)

Unlike conventional triaxial loading, it is clear that brittle failure occurs in the rock samples with unloading failure. As the confining pressure decreases, stress drop occurs rapidly after the peak strength, and internal stored energy is released quickly. Elastic strain energy and dissipated strain energy are no longer gradual processes, but rather sharp increase processes. Elastic strain energy is significantly reduced, while dissipated strain energy is instantly and sharply increased to the total strain energy value.

### DETERMINATION OF MARBLE FAILURE POSITION

In both the conventional triaxial loading test and unloading test, the failure points occur posterior to the peak strength. How to determine the failure point is a matter which requires in-depth discussion. As viewed from the energy conversion relationship in the rock failure process, the energy dissipation process is associated with the entire process of rock deformation, thus resulting in rock failure. The change rate of dissipated energy is used to determine the position of the failure point. The slipping point regression analysis method is used [20], and the first-order derivative of dissipated energy against strain is taken to express the change rate of dissipated energy  $\delta U^d$ :

$$dU^d / d\varepsilon = \delta U^d \tag{2}$$

where  $dU^d$  is the dissipated energy increment,  $d\varepsilon$  is the strain increment corresponding to  $dU^d$  and  $\delta U^d$  is the change rate of dissipated energy. The slipping point regression method is used to take a calculated interval for linear regression at each dissipated energy-strain point, so as to obtain the slope of the interval represented by the point, and then the curves of the relationship between slope and strain at each point are prepared (Fig. 4).

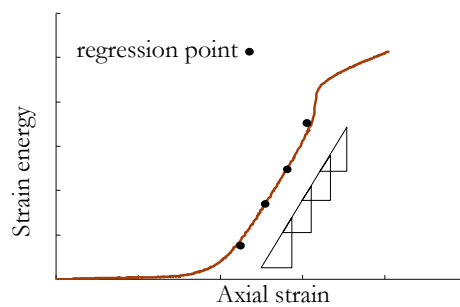


Figure 4: Slipping point regression method [13].

The relation between the change rate of dissipated strain energy and strain at different stress paths is shown in Fig. 5. For the loading test, dissipated strain energy is increased slowly in the compaction and elastic stages, and the change rate of the dissipated strain energy is very small. In the plastic deformation stage, the change rate of the dissipated strain energy is increased, gradually approaching the linear growth law. After the peak to the stress drop stage, the change rate of dissipated energy shows a non-linear growth, then sharply increases to the extreme point at the drop point, leading to rock macroscopic failure plane connected, i.e. the failure point.

Similar to the loading test, the change rate of dissipated strain energy in the unloading test is maintained at a constant level before unloading. The change rate of dissipated strain energy at the unloading position is slightly jumping. Due to changes of stress path, the rock stress state is changed, leading to change in the allocation of absorbed total strain energy, which corresponds to the growth rates of elastic strain energy and dissipated strain energy. The change rate of dissipated strain energy is slowly increased between the unloading point and peak point, then it suddenly increases at the stress drop point. This sudden increase in the change rate of dissipated strain energy indicates a sudden release of stored elastic strain energy, thus leading to rock failure. As viewed from the stress-strain relationship, the sudden change point corresponds to the stress drop point, i.e. the failure point.

It should be noted that for the rock samples with the unloading rate of confining pressure equal to 0.8 MPa/s, a second stress drop exists, and the change rate of dissipated strain energy also shows a small sudden jump at the initial drop point, indicating that partial failure occurs to the rock mass at the stress position, and this sudden jump value is significantly smaller than that at the final failure.

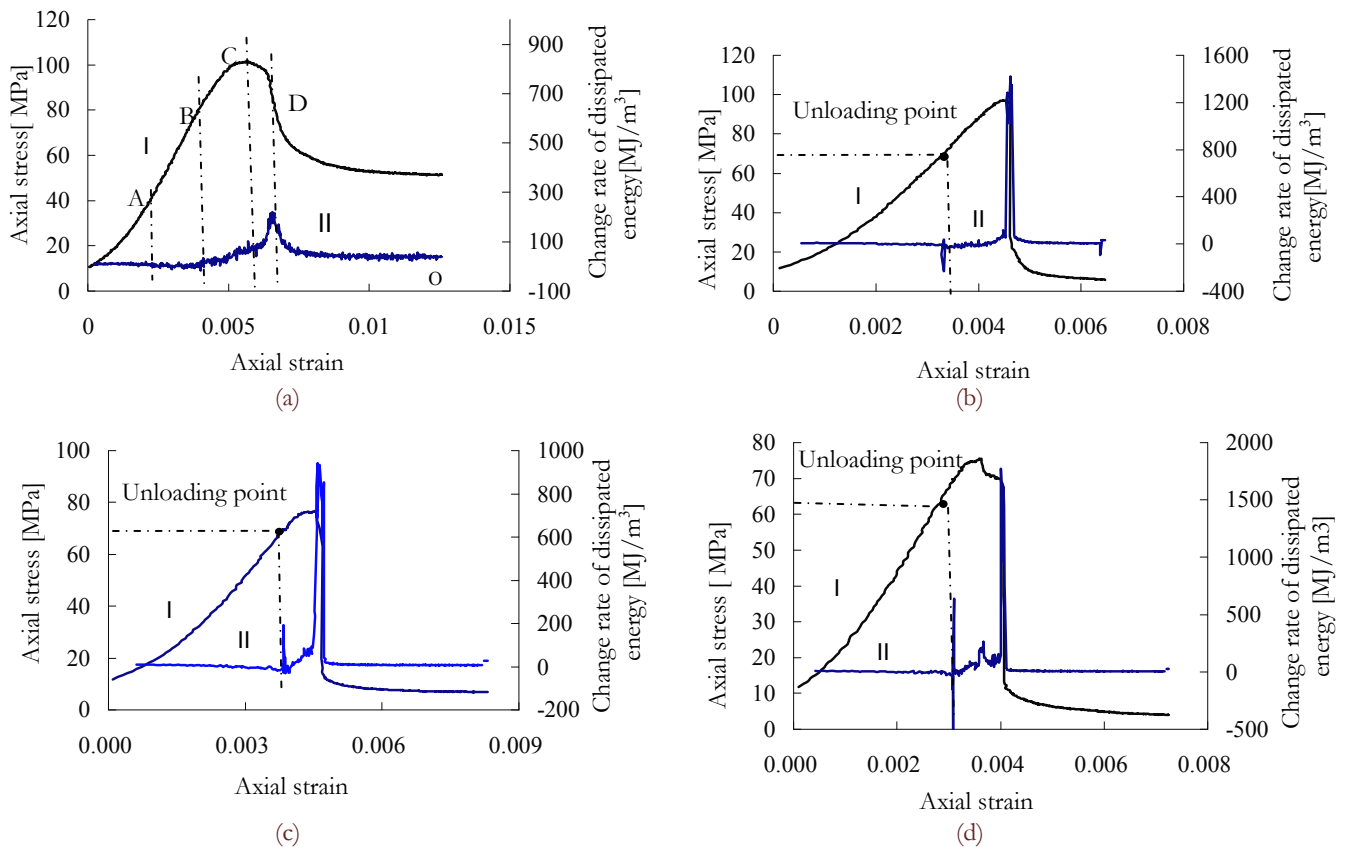


Figure 5: Change rate of dissipated energy of different stress paths: (a) The conventional triaxial loading test; (b) Unloading rate of confining pressure 0.2 MPa/s; (c) Unloading rate of confining pressure 0.4 MPa/s; (d) Unloading rate of confining pressure 0.8 MPa/s (I Axial stress, II Change rate of dissipated strain energy).

The change rate of dissipated strain energy can be used not only to distinguish the various stages of the marble deformation process, but also to determine the position of the failure point, which is a new method that may be used to determine the failure point. The position of the first sudden jump point in the change rate of energy is the unloading point, and the greatest sudden jump point represents the overall failure of the rocks. The stage with a constant change rate of dissipated strain energy is the elastic stage, while that with a growth trend is the plastic stage.

### DEFINITION OF FAILURE VARIABLE

Energy dissipation is achieved through internal crack propagation and failure surface friction, and this process is directly related to rock failure [17]. Therefore, the extent of rock damage is characterized from the perspective of dissipated energy, so as to define the damage variable  $D$  as follows:

$$D = U^d / U \quad (3)$$

The change law of damage variable over axial strain under different confining pressures is shown in Fig. 6. For the loading test, the change in dissipated strain energy is very small in the elastic stage, and the damage variable is basically unchanged. In the plastic deformation stage, the damage variable is increased as the strain grows, and the curve slope gradually increases, which is a gradual process. After the peak strength point, the slope becomes smaller. Between the peak strength point and failure point, the damage variable curve is concave. After rock failure, the damage variable remains constant in the residual deformation stage.

Unlike the damage variable of the loading test, the change of the damage variable is very small in the initial stages after unloading. The damage variable is only rapidly increased when approaching the peak strength point, which is a sudden

increase process. Posterior to the peak strength point of the rock sample in the unloading test, it soon reaches the failure point. After the peak strength point in the loading test, the failure of the rock sample only occurs after the generation of large deformation. It will be a long period of time from the peak strength point to the failure point, and unloading failure is characterized by more sudden occurrence than loading failure.

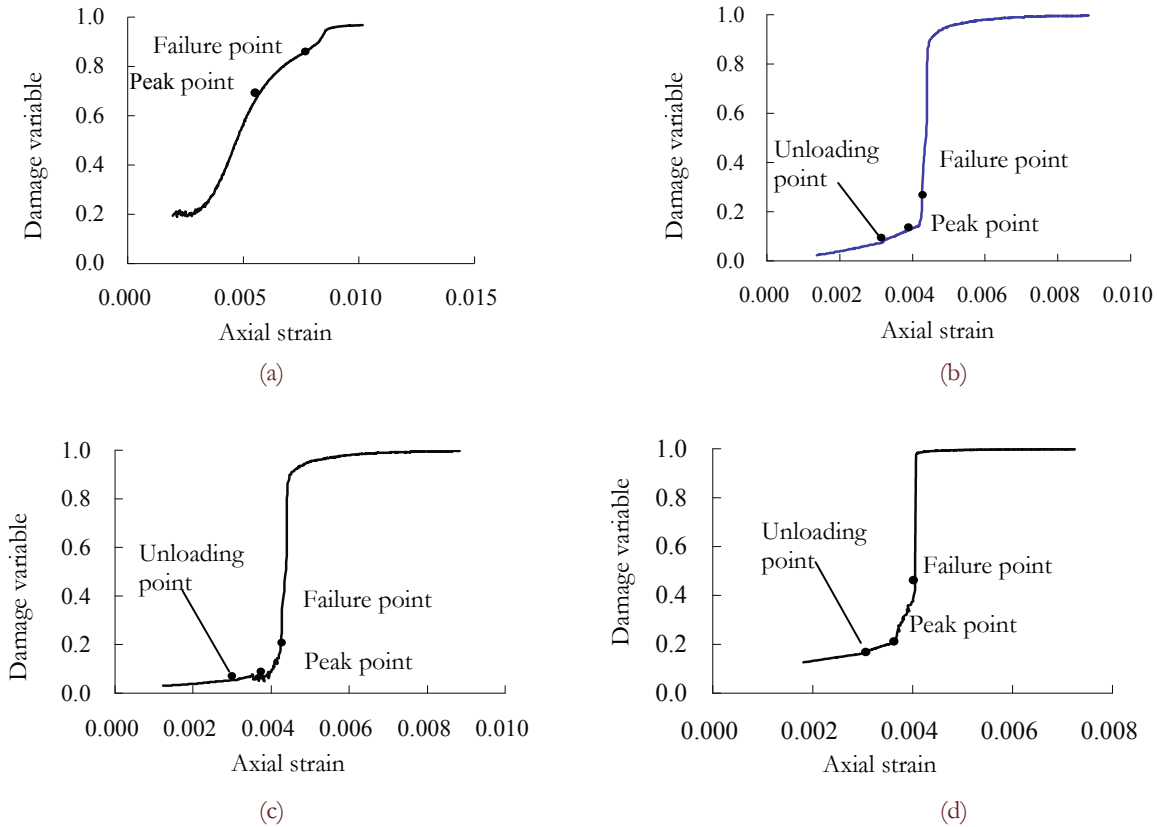


Figure 6: Change of damage variable at different stress paths: (a) The conventional triaxial test; (b) Unloading rate of confining pressure 0.2 MPa/s; (c) Unloading rate of confining pressure 0.4 MPa / s; (d) Unloading rate of confining pressure 0.8 MPa/s.

The deformation control mode is used in the test, and the strain is a constant in the unit of time, i.e.:

$$d\varepsilon / dt = C \tag{4}$$

and

$$\frac{dD}{dt} = \frac{dD}{d\varepsilon} \frac{d\varepsilon}{dt} \tag{5}$$

Eq. (4) is then substituted into Eq. (5), as follows:

$$\frac{dD}{dt} = C \frac{dD}{d\varepsilon} \tag{6}$$

Eq. (6) shows that the damage variable is proportional to the time evolution rate and it is similar to the strain evolution rate. It is indicated that for the deformation control mode with a constant strain rate, the evolutionary law of the damage variable over time may be speculated according to its evolutionary law over strain, which is of reference value to the study of rock creep failure.



## FAILURE CONSTITUTIVE EQUATION

### *Change law of elastic modulus over confining pressure*

Rock mass is a type of non-continuous and non-homogeneous material, the interior of which contains both large and small cracks. In the rock compression process, the increase of confining pressure may improve the crack closure rate, as well as the rock compressive strength and the elastic modulus. Under high confining pressure, the occurrence of slipping requires a large external force, so that the rock strength is higher and the elastic modulus is greater. Considering the impact of confining pressure on the elastic modulus, it is found, by fitting the experimental data, that the elastic modulus is closely related to the confining pressure, and the change law is shown as below:

$$E_r = E_1 \left\{ 1 + c \left[ \exp \left( \frac{a\sigma_3}{E_1} \right) - 1 \right] \right\} \quad (7)$$

where  $E_r$  is the elastic modulus after confining pressure correction,  $E_1$  is the elastic modulus under uniaxial compression, and  $E_r = E_1$  in the uniaxial loading test. In addition,  $a$  is the correction coefficient of the curve peak, and  $c$  is a parameter used to characterize the change rate of the confining pressure.  $c$  is equal to 1 in the conventional triaxial test, while  $c$  is changed over the confining pressure in the unloading test.

### *Establishment of constitutive equation*

The rock itself is shown to contain certain initial damage. According to Eq. (7), rock damage will be increased with higher dissipated strain energy in the compression process. Assuming that the rock stress has a power function relationship with the damage variable, the elastic modulus after the confining pressure correction is used to establish the damage constitutive equation:

$$\sigma = E(1 - D)^b \varepsilon \quad (8)$$

Eq. (7) is then substituted into Eq. (8), so to obtain:

$$\sigma = E_1 \left\{ 1 + c \left[ \exp \left( \frac{a\sigma_3}{E_1} \right) - 1 \right] \right\} (1 - D)^b \varepsilon \quad (9)$$

where  $b$  is the correction coefficient of curve shape.

Taking the conventional triaxial loading test data as an example (confining pressure: 10 MPa), the impact of the Eq. (9) parameters on the stress-strain curve distribution characteristics is analyzed. Fig. 7 shows the stress-strain curve by assuming  $b$  equal to 0.5 and different values for parameter  $a$ . As the value of  $a$  increases, steeper pre-peak curve, higher peak strength and smaller residual strength can be observed, thus indicating that  $a$  is correlated with the compressive strength. Under the same stress, the greater the  $a$  value is, the smaller the pre-peak deformation will be, so the  $a$  value also reflects the rock deformation characteristics.

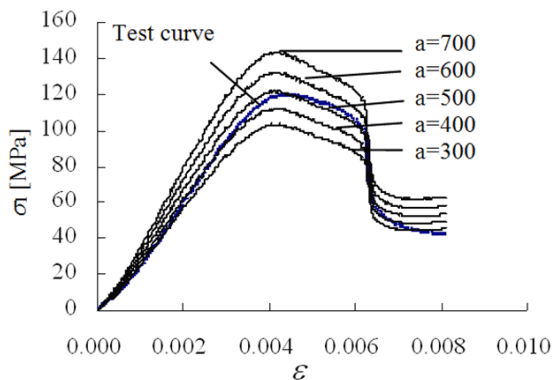


Figure 7: Stress-strain curves of different parameter  $a$  ( $b=0.5$ ).

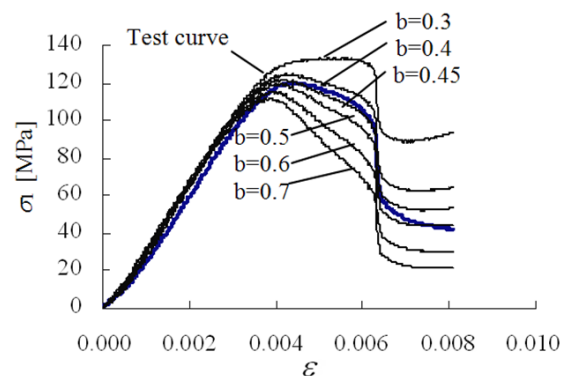


Figure 8: Stress-strain curves of different parameter  $b$  ( $a=500$ ).



Fig. 8 shows the stress-strain curve obtained by assuming  $a$  equal to 500 and by varying  $b$  value. The  $b$  value has little effect on the pre-peak stage, and the various curves are basically overlapped. A smaller  $b$  value determines a slightly higher peak strength. On the contrary, it has a greater impact on post-peak softening and on the residual strength of the rock. The greater the  $b$  value is, the more significant the post-peak strain softening phenomenon of the rock sample will be, and the smaller the residual strength will be.  $b$  has a great impact on the curve shape between the peak strength and the stress drop point. Rock has a plastic flow tendency with the reduction of  $b$  while it shows a significant brittle stress drop with the increase of  $b$ .

Stress path	Confining pressure [MPa]	Unloading rate [MPa/s]	$a$	$b$	$c$	R <sup>2</sup> (%)
The conventional triaxial test	10		427	0.36		98
	20		442	0.38	1	97
	30		468	0.41		95
	40		500	0.45		94
Unloading test		0.2	1.2052	0.5022	320.36	98
	10	0.4	1.2164	0.5059	338.32	97
		0.8	1.2850	0.4938	332.19	97
		0.2	1.1320	0.5385	310.12	99
	20	0.4	1.2540	0.5382	324.50	99
		0.8	1.0350	0.7922	342.50	90
		0.2	0.9735	0.7860	345.80	99
	30	0.4	0.9509	0.7120	333.64	98
		0.8	0.8321	0.7226	373.89	98
		0.2	0.8635	0.6894	342.5	98
	40	0.4	0.8456	0.7011	368.32	97
		0.8	0.8247	0.7376	328.47	98

Table 1: Parameter value setting

Based on the test data, the parameters, i.e.  $a$ ,  $b$  and  $c$ , are adjusted to simulate the constitutive equation, and the Matlab nonlinear fitting tool is used to perform test data regression. Tab. 1 lists the parameters, i.e.  $a$ ,  $b$  and  $c$ , under different stress paths. Figs. 9 and 10 show the fitting curves of the constitutive equation on the conventional triaxial loading and unloading tests, respectively. The stress-strain curve simulated by this constitutive equation is highly consistent with the experimental curve, with a correlation coefficient greater than 94%.

The internal cracks caused by rock compression are closed, so that an initial compression stage will likely exist in the stress-strain curve. The initial stage of the stress-strain curve simulated by this constitutive equation can reflect the concave shape of the curve in the compaction stage. Under static loading conditions, the rocks are loaded from the initial state to the failure process, i.e. internal crack compaction, fissure propagation, aggregation and connection, which is a continuous process, so that the entire process of stress-strain equation becomes unified. In this study, a unified equation is used to simulate the deformation process, so as to avoid the shortcomings of staged fitting. This constitutive equation considering the confining pressure impact contains only three parameters. Through adjusting these three parameters, the rock deformation processes under various stress paths may be simulated, thus this model is highly adaptable.

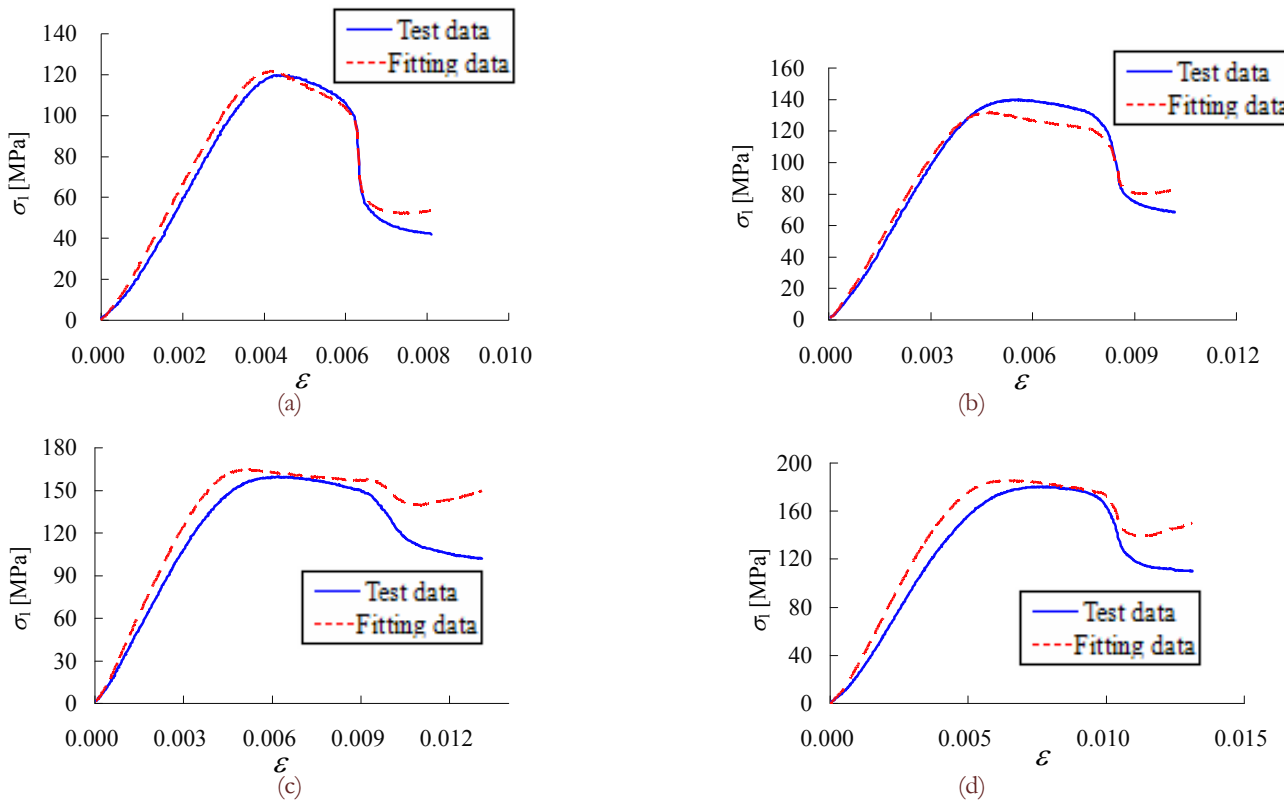


Figure 9: Stress-strain curves of conventional triaxial tests: (a) Confining pressure 10 MPa; (b) Confining pressure 20 MPa; (c) Confining pressure 30 MPa; (d) Confining pressure 40 MPa.

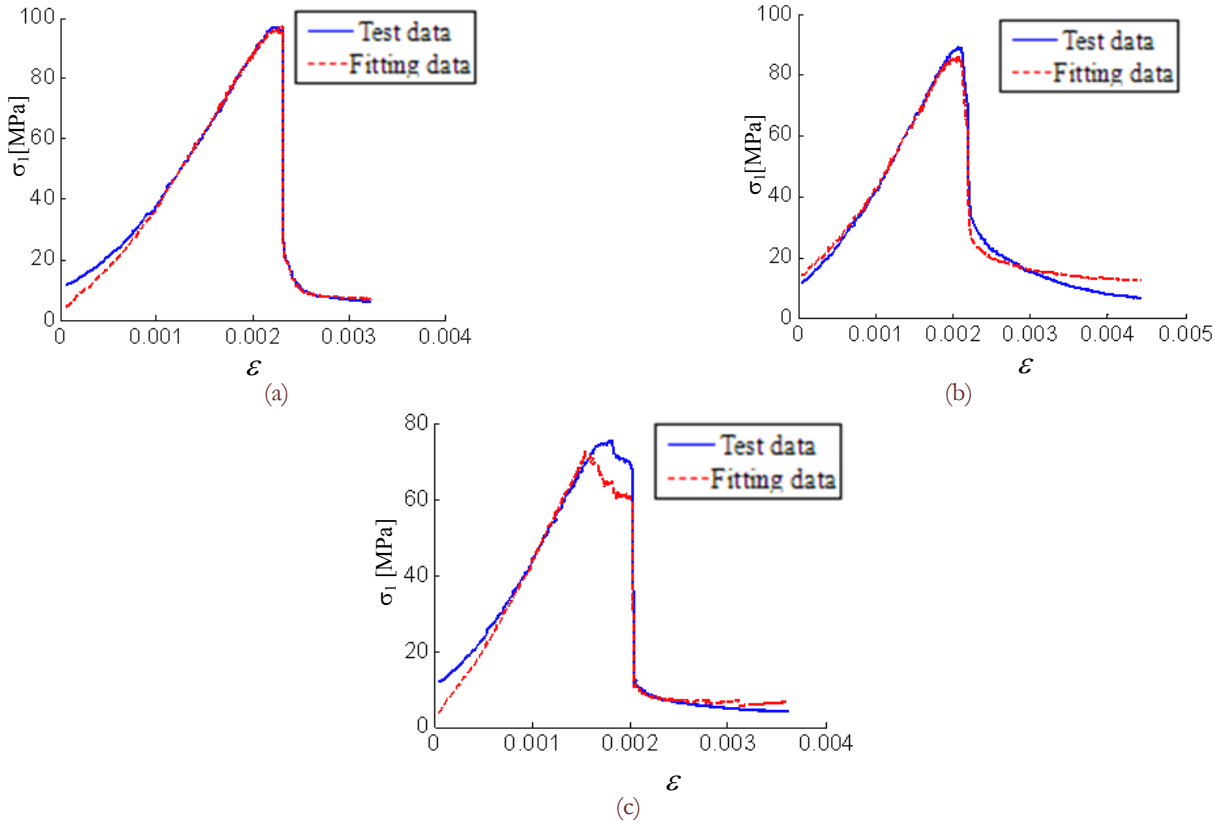


Figure 10: Stress-strain curves of different unloading rates: (a) Unloading rate of confining pressure 0.2 MPa/s; (b) Unloading rate of confining pressure 0.4 MPa/s; (c) Unloading rate of confining pressure 0.8 MPa/s.



## CONCLUSIONS

The energy dissipation process is associated with the entire process of rock deformation, thus resulting in rock failure. The compaction and elastic stages mainly form the accumulation process of elastic strain energy. After the peak strength, dissipated strain energy is increased significantly. In the unloading test, the elastic strain energy is released at the stress drop point, while the dissipated strain energy increases sharply.

The change rates of dissipated strain energy can be used not only to distinguish the various stages of deformation process, but also to determine the position of the failure point. The stage with a constant change rate of energy is the elastic stage, while that with a growth trend is the plastic stage.

The ratio between dissipated strain energy and total strain energy is defined as the damage variable. The change of damage variable is a gradual process for the conventional triaxial loading test, while it is a sudden increase process for the unloading test. The damage mechanics model in the marble deformation process is established from the perspective of energy dissipation, which may reflect the impacts of confining pressure changes on the marble strength.

## ACKNOWLEDGEMENT

The study is supported by the National Natural Science Foundation of China (41472270, 41372298), Shandong Province Higher Educational Science and Technology Program (J10LE01) and Qingdao Science and Technology Program (12-1-4-4-(10)-jch).

## REFERENCES

- [1] Cao, W., G., Zhang, S., Zhao, M., H., Study on statistical damage constitutive model of rock based on new definition of damage, *Rock and Soil Mechanics*, 27(1)(2006) 41-46.
- [2] Qin, Y., P., Zhang, J., F., Wang, L., Preliminary discussion on theoretical model of rock damage mechanics, *Chinese Journal of Rock Mechanics and Engineering*, 22(4) (2003) 646-650.
- [3] Ha, Q., L., Rock slope engineering and unloading nonlinear rock mass mechanics, *Chinese Journal of Rock Mechanics and Engineering*, 16(4)(1997)386-391.
- [4] Huang, R., Q., Huang, D., Experimental research on mechanical properties of granites under unloading condition, *Chinese Journal of Rock Mechanics and Engineering*, 27(11) (2008) 2205-2213.
- [5] Huang, D., Huang, R., Q., Zhang, Y., X., Experimental investigations on static loading rate effects on mechanical properties and energy mechanism of coarse crystal grain marble under uniaxial compression, *Chinese Journal of Rock Mechanics and Engineering*, 31(2) (2012) 245-255.
- [6] Wu, Z., Zhang, C., J., Unidirectional loading and mechanical damage model of rock properties, *Chinese Journal of Rock Mechanics and Engineering*, 15(1) (1996) 55-61.
- [7] Shi, C., Jiang, X., X., Zhu, Z., D., et al., Study of rock damage age constitutive model and discussion of its parameters based on Hoek-Brown, *Chinese Journal of Rock Mechanics and Engineering*, 30(1) (2011) 2647-2652.
- [8] Zhang, Q., S., Yang, G., S., Ren, J., X., New study of damage variable and constitutive equation of rock, *Chinese Journal of Rock Mechanics and Engineering*, 22(1) (2013) 30-34.
- [9] Xu, W., Y., Wei, L., D., Study on statistical damage constitutive model of rock, *Chinese Journal of Rock Mechanics and Engineering*, 21(6) (2002) 787-791.
- [10] Chen, W., Z., Lu, S., P., Guo, X., H., et al., Research on unloading confining pressure tests and rock burst criterion based on energy theory, *Chinese Journal of Rock Mechanics and Engineering*, 28(8) (2009) 1530-1540.
- [11] Xu, G., A., Niu, S., J., Jing, H., W., et al., Experimental study of energy features of sandstone under loading and unloading, *Rock and Soil Mechanics*, 32(12) (2011)3611-3617.
- [12] Jin, F., N., Jiang, M., R., Gao, X., L., Defining damage variable based on energy dissipation, *Chinese Journal of Rock Mechanics and Engineering*, 23(12) (2004) 1976-1980.
- [13] Du, W., The isotropic damage constitutive model based on the principle of energy dissipation, *Journal of Sichuan building*, 30(2) (2010) 183-185.
- [14] Hua, A., Z., You, M., Q., Rock failure due to energy release during unloading and application to underground rock burst control, *Tunnelling and Underground Space Technology*, 16(3) (2001) 241-246.



- [15] Zhou, X., P., Yang, H., Q., Zhang, Y., X., Rate dependent critical strain energy density factor of Huanglong limestone, *Theoretical and Applied Fracture Mechanics*, 51(1) (2009) 57-61.
- [16] Gaziev, E., Rupture energy evaluation for brittle materials, *International Journal of Solids and Structures*, 38(42-43) (2001) 7681-7690.
- [17] Xie, H., P., Ju, Y., Li, L., Y., Criteria for strength and structural failure of rocks based on energy dissipation and energy release principles, *Chinese Journal of Rock Mechanics and Engineering*, 24(17) (2005) 3003-3010.
- [18] Liu, X.,M., Xiong, L., Liu, J.,H., et al, Slacking mechanism of red sandstone based on energy dissipation principle, *Journal of Central South University (Science and Technology)*, 42(10) (2011) 3143-3149
- [19] Zhang, X., Y., Cheng, J., Kang, Y., H., et al, Analysis on damage and energy during rock deformation under cyclic loading and unloading conditions, *Nonferrous Metals*, 63(5) (2011) 41-45.
- [20] Eberhardt, E., Stead ,D., Stimpson, B., et al, Identifying crack initiation and propagation thresholds in brittle rock, *Canada Geotechnical Journal*, 35 (1998) 222-233.